

## Threshold switching behavior of Ag-Si based selector device and hydrogen doping effect on its characteristics

Jongmyung Yoo, Jiyong Woo, Jeonghwan Song, and Hyunsang Hwang

Citation: *AIP Advances* **5**, 127221 (2015); doi: 10.1063/1.4938548

View online: <http://dx.doi.org/10.1063/1.4938548>

View Table of Contents: <http://aip.scitation.org/toc/adv/5/12>

Published by the [American Institute of Physics](#)

---

### Articles you may be interested in

[Dynamics of electroforming and electrically driven insulator-metal transition in NbOx selector](#)

*AIP Advances* **108**, 232101232101 (2016); 10.1063/1.4953323

[Comprehensive scaling study of NbO2 insulator-metal-transition selector for cross point array application](#)

*AIP Advances* **108**, 153502153502 (2016); 10.1063/1.4945367

[Bidirectional threshold switching in engineered multilayer \(Cu2O/Ag:Cu2O/Cu2O\) stack for cross-point selector application](#)

*AIP Advances* **107**, 113504113504 (2015); 10.1063/1.4931136

[Access devices for 3D crosspoint memory](#) Some portions of this review article will appear in G. W. Burr, R. S. Shenoy, and H. Hwang, "Select device concepts for crossbar arrays," in *Resistive Switching—From Fundamentals of Nanoionic Redox Processes to Memristive Device Applications*, edited by D. Ielmini and R. Waser (in press), Chap. 23. Copyright Wiley-VCH Verlag GmbH & Co. KGaA. Reproduced with permission.

*AIP Advances* **32**, 040802040802 (2014); 10.1116/1.4889999

---

# HAVE YOU HEARD?

Employers hiring scientists and engineers trust

**PHYSICS TODAY | JOBS**

[www.physicstoday.org/jobs](http://www.physicstoday.org/jobs)



## Threshold switching behavior of Ag-Si based selector device and hydrogen doping effect on its characteristics

Jongmyung Yoo, Jiyong Woo, Jeonghwan Song, and Hyunsang Hwang<sup>a</sup>

*Department of Materials Science and Engineering, Pohang University of Science and Technology (POSTECH), 77 Cheongam-ro, Nam-gu, Pohang, 790-784, Republic of Korea*

(Received 18 October 2015; accepted 9 December 2015; published online 18 December 2015)

The effect of hydrogen treatment on the threshold switching property in a Ag/amorphous Si based programmable metallization cells was investigated for selector device applications. Using the Ag filament formed during motion of Ag ions, a steep-slope (5 mV/dec.) for threshold switching with higher selectivity ( $\sim 10^5$ ) could be achieved. Because of the faster diffusivity of Ag atoms, which are inside solid-electrolytes, the resulting Ag filament could easily be dissolved under low current regime, where the Ag filament possesses weak stability. We found that the dissolution process could be further enhanced by hydrogen treatment that facilitated the movement of the Ag atoms. © 2015 Author(s). All article content, except where otherwise noted, is licensed under a Creative Commons Attribution (CC BY) license (<http://creativecommons.org/licenses/by/4.0/>). [<http://dx.doi.org/10.1063/1.4938548>]

Resistive random access memory (RRAM) is one of the most promising emerging nonvolatile memories owing to its excellent scalability, fast operation, low power consumption, and relatively simple fabrication process.<sup>1</sup> For ultra-high integration density, passive cross-point array is the most attractive architecture. In this architecture, however, it is essential to suppress the sneak current from the neighboring cells that can reduce the readout sense margin, increase the power consumption and limit the array size.<sup>2</sup> One way to suppress the sneak current is to use RRAMs with self-rectification property as one resistor (1R) configuration since the rectifying characteristics can significantly reduce the leakage current flowing through a reverse-biased RRAM cell, and various types of rectifying RRAM devices have been demonstrated.<sup>3-5</sup> An alternative method is to connect a nonlinear circuit element such as a selector device to each RRAM cell as one selector and one resistor 1S-1R configuration. Several selector devices such as tunneling diodes,<sup>6</sup> bidirectional varistors,<sup>7</sup> mixed-ionic-electronic-conduction (MIEC),<sup>8</sup> Ovonic threshold switching (OTS)<sup>9</sup> and metal-insulator transition (MIT) have been proposed.<sup>10</sup> However, these selector devices cannot sufficiently suppress the leakage current, which is required for achieving high density RRAM integration. To solve this high leakage current problem, a bipolar threshold switching selector device was reported that had selectivity  $>10^7$ , ultra-low off current  $<100$  pA, and steep turn-on slope  $<5$  mV/decade.<sup>11</sup> However, important information about the selector device such as materials and operating mechanism of the device were not disclosed.

In this study, we show that threshold switching behaviors with desired properties such as ultra-low off current of  $<100$  pA and steep turn-on slope of 5 mV/decade can be obtained in a carefully engineered Ag/amorphous Si (a-Si) based programmable metallization cell (PMC) device. The mechanism of PMC device involves formation and rupture of metal filaments in an electrolyte owing to the electrochemical reactions. By adopting Ag-Si system where the Ag atoms have high diffusivity, we can reduce the stability of the metal filament and hence obtain threshold switching characteristics at higher  $I_{\text{comp}}$ , which has been normally reported at low  $I_{\text{comp}}$  as  $\leq 100$  nA.<sup>12,13</sup> In addition, by enhancing diffusivity of the Ag atoms and removing leakage paths in the a-Si film of the device through hydrogen doping of the a-Si layer, we can induce a faster dissolution of the metal filament and lower down the off current of the device.

<sup>a</sup>Author to whom correspondence should be addressed. Electronic mail: [hwanghs@postech.ac.kr](mailto:hwanghs@postech.ac.kr)

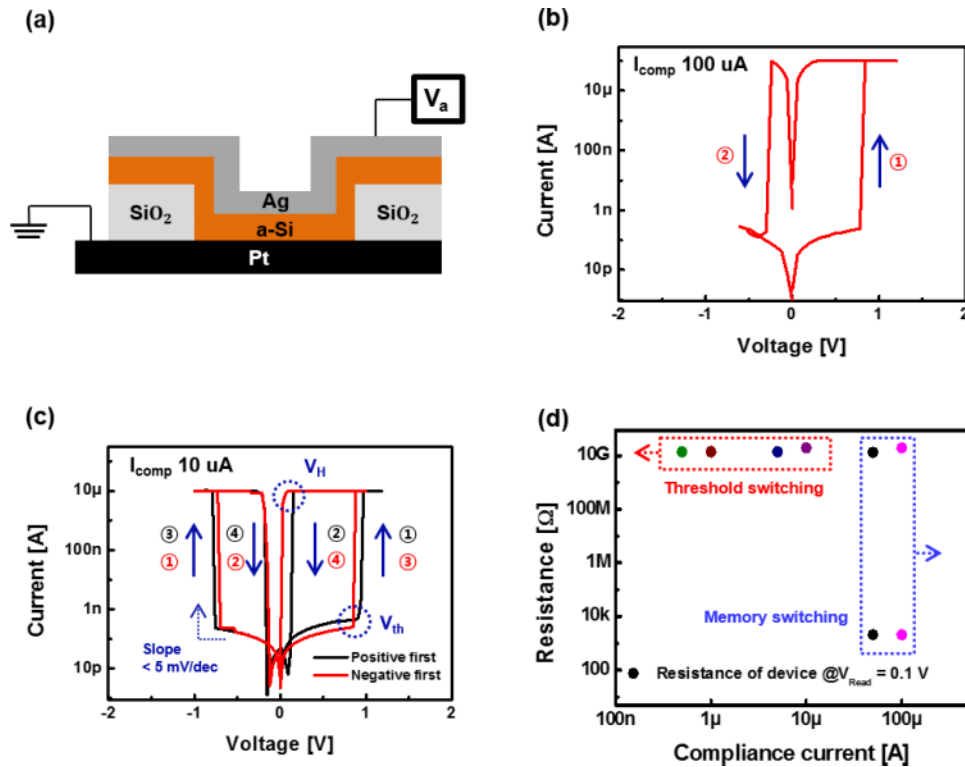


FIG. 1. (a) A schematic diagram of Ag/a-Si/Pt stacked 250 nm via-hole selector device. Compliance current dependent (b) memory switching and (c) threshold switching characteristics of Ag/a-Si based selector device. (d) Read resistances following SET/ON operation at various compliance currents.

We fabricated an Ag/Silicon-based PMC device with a via-hole structure, as illustrated in Fig. 1(a). A 100-nm-thick SiO<sub>2</sub> layer was deposited on a Pt bottom electrode (BE) substrate through plasma-enhanced chemical vapor deposition for the isolation layer. Subsequently, 250 nm via holes were patterned using lithography and reactive ion etching processes. Then, a 10-nm-thick amorphous Si layer and a 5-nm-thick Ag top electrode (TE) layer was deposited by sputtering system under pure Ar ambient gas in a sequence at room temperature.

The as-fabricated devices with Ag/a-Si/Pt stack were in the high resistance state (HRS) with an extremely low current level near 100 pA at a read voltage of 0.1 V, and the current-voltage (I–V) characteristics showed memory switching at 100 μA, as illustrated in Fig. 1(b). As the positive voltage bias was swept to ~0.8 V, the HRS current suddenly increased from 100 pA to I<sub>comp.</sub>(100 μA) and changed to a low resistance state (LRS), which corresponds to the SET operation. This LRS was retained even after the removal of the applied bias. When the voltage was swept to a negative polarity, a dramatic current drop was observed at ~-0.3 V that corresponds to the RESET operation. On the contrary, threshold switching was observed at a lowered I<sub>comp.</sub> of 10 μA, which is shown in Fig. 1(c). When the voltage bias higher than a certain voltage called threshold voltage ( $\pm V_{th} \pm 0.8$  V) was applied, the initially low current (100 pA) abruptly jumped to I<sub>comp.</sub> (10 μA) and the device suddenly switched to the ON state. However, compared to the device operating at 100 μA, this device could not remain in the ON state such that when the applied bias was decreased back to a certain value called hold voltage ( $\pm V_H \cong \pm 0.1$  V), the device readily went back to HRS (OFF state). This observed transition from memory switching to threshold switching with decrease of the current was also confirmed by comparing the resistances at 0.1 V before and after SET/ON operation at various compliance currents, as shown in Fig. 1(d).

The observed behaviors in the Ag/a-Si based PMC device are schematically described in Fig. 2. When a positive bias was applied, Ag ions can be ionized from the Ag TE as an ion source, and then the Ag ions can migrate toward the BE. As a result, the metallic filament whose size is dependent on

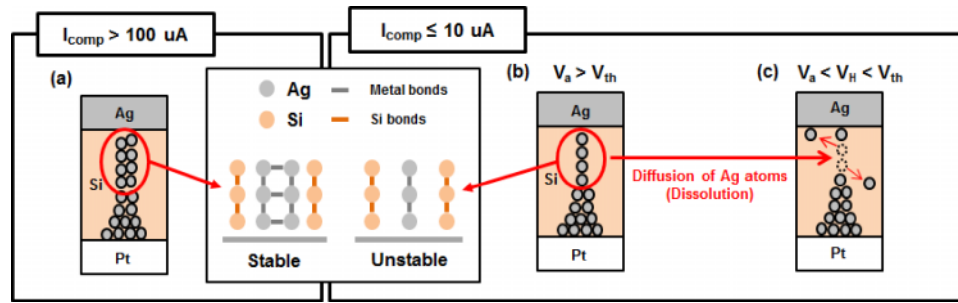


FIG. 2. Schematic diagrams explaining switching characteristics of Ag/a-Si based PMC device at different current compliances. (a) Stable thick filament formed at high  $I_{comp} (>100 \mu A)$  results in memory switching. (b) Unstable thin filament formed at low  $I_{comp} (\leq 10 \mu A)$  and (c) high diffusivity of the Ag atoms in a-Si result in spontaneous rupture of the filament and hence the threshold switching.

$I_{comp}$  values was formed by electrochemical reaction.<sup>14</sup> Under high  $I_{comp}$  as  $>100 \mu A$ , the formation of thicker filament was preferred because of the supplied large amount of Ag ions from the TE, as shown in Fig. 2(a). This thick filament was stable because it had plenty of metal-metal bonds that strongly tied the Ag atoms composing the filament together.<sup>15</sup> Therefore, the state of filament can be maintained even after the removal of the voltage bias, thereby showing memory switching behavior. On the other hand, when the set  $I_{comp}$  was lowered down to  $\leq 10 \mu A$ , a smaller size of filament composed of a few Ag ions was formed, which is illustrated in Fig. 2(b). Because this reduced size of filament consisted of less metal bonds, the force to tie the metal atoms together was diminished. Therefore, when the voltage bias was removed, the Ag atoms composing the filament became easier to be moved by diffusion through defect sites, which is schematically described in Fig. 2(c). The atomistic diffusion of the Ag atoms outside its original position in the filament indicates its dissolution. Thus, if the metal atoms have high diffusivity in the electrolyte, fast dissolution of the metal filament (that resulted by fast diffusion of the surface atoms) can occur, thereby exhibiting threshold switching behavior. The diffusivity of the metal atoms in an amorphous matrix can be explained by an interstitial diffusion equation following Arrhenius law because most transition metals mainly diffuse through interstitial sites.<sup>16</sup> The interstitial diffusion equation is as follows

$$D_i^* = D_{i,0}^* \exp[-(H_i^M + H_{it}^B)/kT]$$

The quantities  $D_i^*$ ,  $D_{i,0}^*$ ,  $H_i^M$  and  $H_{it}^B$  represent the effective interstitial diffusivity, pre-exponential factor, migration enthalpy for the interstitial atoms, and binding enthalpy of traps which capture diffusing metal atoms, respectively. According to the equation, metal atoms can diffuse out fast if their migration enthalpy and number of the traps in electrolytes is small. In case of Ag/a-Si based PMC device, Ag atoms had high diffusivity in a-Si layer because of their low migration enthalpy in the electrolyte and thus threshold switching was resulted in the device.<sup>17</sup> In addition, switching to the ON state in the negative polarity was possible in this device because the Ag metal deposited by sputtering system penetrated into the Si layer during the fabrication process. To prove the incorporation of Ag into the a-Si layer, we used HR-TEM based images and Energy Dispersive Spectroscopies (Not shown here). The amount of Ag inside the a-Si layer was calculated to be about 5.80 atomic % according to the EDS analysis. This injected Ag atoms can be served as ion sources which result in the bi-directional switching behavior of the device.

As abovementioned, the diffusivity of Ag atoms, the driving force to dissolve the filament, can be further increased by reducing the number of trapping sites in the amorphous electrolyte. Therefore, to induce even faster dissolution of the filament, we doped the amorphous Si layer using hydrogen, which is one of the methods to remove traps in the a-Si film.<sup>18</sup> The hydrogen doping of the amorphous Si layer was performed by replacing pure Ar ambient gas to Ar + H<sub>2</sub> forming gas with 5% hydrogen ratio in the Si sputtering process. Hydrogen contained in the forming gas can be incorporated into the a-Si film with the assist of plasma during the sputtering process.<sup>19</sup> Fig. 3(a) shows the I-V characteristics of the hydrogen doped Ag/a-Si (Ag/a-Si:H) system of the device. Compared to the previous device ( $V_H \sim \pm 0.1$  V), a remarkable increase in the  $|\pm V_{hold}|$  was clearly

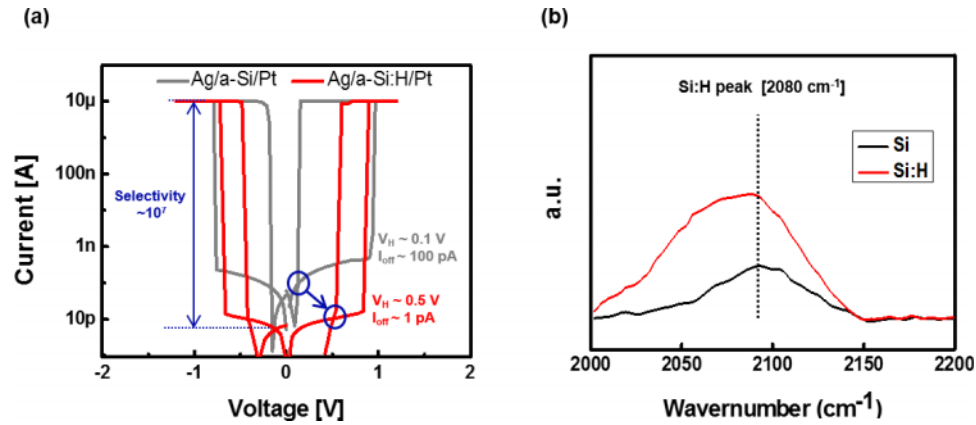


FIG. 3. (a) Comparison of I-V characteristics of Ag/a-Si with and without hydrogen doping process. (b) FT-IR plot of two samples; red curve is for a sample with hydrogen doping and black curve is for a sample without hydrogen doping.

observed in the hydrogen doped device ( $V_H \sim \pm 0.5$  V). Moreover, a decreased off state current and thus an increased selectivity from  $10^5$  to  $10^7$  were observed. We believed that the hydrogen treatment contributed to the changes in the electronic characteristics of the device, and the effect of hydrogen on the Si film was analyzed by Fourier Transform Infrared (FTIR) spectroscopy. Fig 3(b) shows FTIR spectra of two samples, one deposited without hydrogen doping (black) and one with the hydrogen doping (red). In the spectroscopy, a peak difference was clearly detected at  $2080\text{ cm}^{-1}$ . This result indicates that the hydrogen-doped device has Si film passivated by hydrogen because a peak at  $2080\text{ cm}^{-1}$  denotes the presence of hydrogen-Si bondings in the film.<sup>19</sup>

The observed changes in the characteristics of the Ag/a-Si:H system of device can be explained as follows. Intrinsic dangling defects existing in the amorphous Si film of the device worked as traps in terms of atomic diffusion and thus impeded their diffusion, which is schematically demonstrated in Fig. 4(a).<sup>16</sup> Because the hydrogen atoms bonded to Si dangling defects, trapping of the metal atoms were prevented, and therefore an uninterrupted fast diffusion was resulted, as schematically described in Fig. 4(b).<sup>20</sup> Faster diffusion of the metal atoms composing the filament led to its faster dissolution. This faster diffusion of metal atoms can be indirectly confirmed by checking the change of  $V_H$ . Not only  $V_H$  was increased but the overall resistance of the selector device was also increased, because of the removal of the defects that caused leakage paths.<sup>20</sup> Thus, the off-state current of the device could be further lowered to  $\sim 1$  pA level, which can expand the maximum array size in the cross-point memory array.

The newly fabricated Ag/a-Si:H system of the device showed good endurance along with excellent switching uniformity. Fig. 5 indicates distribution data based on 100 DC cycles operated in this device. Tight distribution of the off-state current read at  $1/2 V_{th}$ , shown in Fig. 5(a), proves good switching uniformity of the device. Moreover, ensured voltage margin of about 1.4 V was noted in Fig. 5(b) where distribution data of  $V_{th}$  and  $V_H$  is shown.

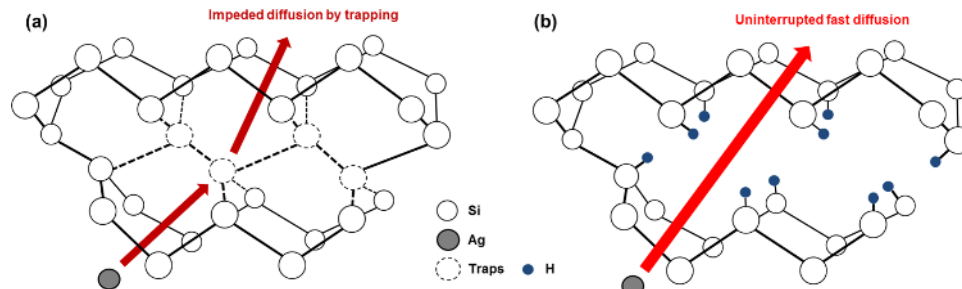


FIG. 4. Schematic diagrams demonstrating (a) impeded diffusion of metal atoms by trapping of Si dangling defects in amorphous Si film and (b) uninterrupted fast diffusion in hydrogen passivated Si layer.

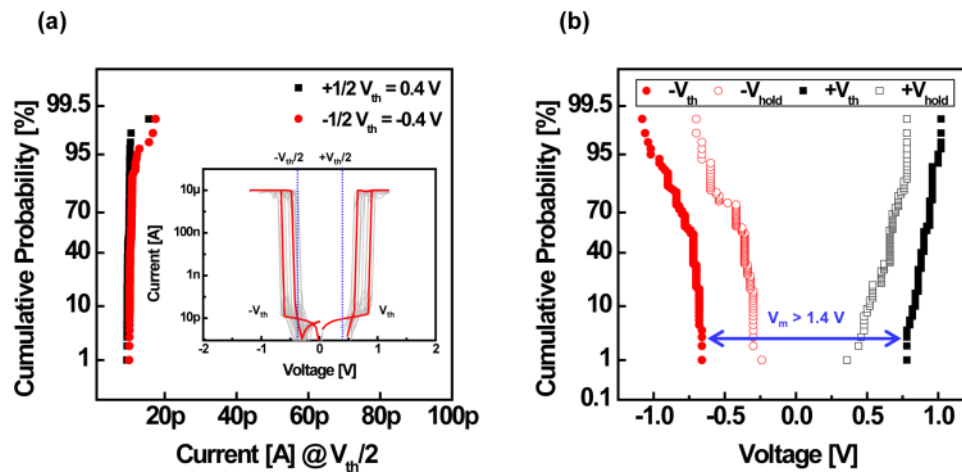


FIG. 5. (a) Cumulative probability of current levels read at half  $V_{th}$ . Inset shows typical I-V characteristics of Ag/a-Si based threshold selector device (100 DC cycles). (b) Cumulative probability of  $V_{th}$  and  $V_{hold}$ .

We have demonstrated a threshold switching selector device with a steep turn-on slope and a high ON current obtained by adopting Ag/a-Si system, where the Ag atoms have high diffusivity, which led to fast dissolution of the metal filament. In addition, through hydrogen doping, we could induce faster dissolution of the metal filament and could lower down off-state current of the device because the doped hydrogen atoms passivated traps in the a-Si film. We hope that this novel approach helps in achieving the future cross-point array applications.

## ACKNOWLEDGEMENTS

This work was supported by the POSTECH-Samsung Electronics ReRAM Cluster Research.

- <sup>1</sup> R. Waser and M. Aono, "Nanoionics-based resistive switching memories," *Nature Mater.* **6**, 833–840 (2007).
- <sup>2</sup> E. Linn, R. Rosezin, C. Kugeler, and R. Waser, "Complementary resistive switches for passive nanocrossbar memories," *Nat. Mater.* **9**, 403 (2010).
- <sup>3</sup> K. Kim, S. Jo, S. Graba, and W. Lu, "Nanoscale resistive memory with intrinsic diode characteristics and long endurance," *Appl. Phys. Lett.* **96**, 053106 (2010).
- <sup>4</sup> X. A. Tran, B. Gao, J. F. Kang, X. Wu, L. Wu, Z. Fang, Z. R. Wang, K. L. Pey, Y. C. Yeo, A. Y. Du, M. Liu, B. Nguyen, M. F. Li, and H. Y. Yu, "Self-rectifying and forming-free unipolar HfO<sub>x</sub> based high performance RRAM built by Fab-Available materials," in IEDM Tech. Dig., Dec. 2011, pp. 31.2.1-31.2.4.
- <sup>5</sup> C. Hsu, I. Wang, C. Lo, M. Chiang, W. Jang, C. Lin, and T. Hou, "Self-rectifying bipolar TaO<sub>x</sub>/TiO<sub>2</sub> RRAM with superior endurance over 10<sup>12</sup> cycles for 3D high-density storage-class memory," in VLSI symp. Tech. Dig., Jun. 2013, pp. T166-T167.
- <sup>6</sup> A. Kawahara, R. Azuma, Y. Ikeda, K. Kawai, Y. Katoh, K. Tanabe, T. Nakamura, Y. Sumimoto, N. Yamada, N. Nakai, S. Sakamoto, Y. Hayakawa, K. Tsuji, S. Yoneda, A. Himeno, K. Origasa, K. Shimakawa, T. Takagi, T. Mikawa, and K. Aono, "An 8Mb Multi-Layered Cross-Point ReRAM Macro with 443MB/s Write Throughput," *IEEE Trans. Electron Devices* **61**(8), 2820–2826 (2014).
- <sup>7</sup> W. Lee, J. Park, J. Shin, J. Woo, S. Kim, G. Choi, S. Jung, S. Park, D. Lee, E. Cha, H. Lee, S. Kim, S. Chung, and H. Hwang, "Varistor-type bidirectional switch ( $J_{Max} > 10^7$  A/cm<sup>2</sup>, Selectivity  $\sim 10^4$ ) for 3D bipolar resistive memory arrays," in Proc. Symp. VLSI Technol., Jun. 2012, pp. 37-38.
- <sup>8</sup> G. W. Burr, K. Virwani, R. S. Sheony, A. Padilla, M. BrightSky, E. A. Joseph, M. Lofaro, A. J. Kellock, R. S. King, K. Nguyen, A. N. Bowers, M. Jurich, C. T. Rettner, B. Jackson, D. S. Bethune, R. M. Shelby, T. Topuria, N. Arellano, P. M. Rice, B. N. Kurdi, and K. Gopalakrishnan, "Large-scale (512kbit) integration of multilayer-ready access-devices based on mixed-ionic-electronic-conduction (MIEC) at 100% yield," in VLSI Symp. Tech. Dig., Jun. 2012, pp. 41-42.
- <sup>9</sup> S. Kim, Y. Kim, K. Kim, S. Kim, S. Lee, M. Chang, E. Cho, M. Lee, D. Lee, C. Kim, U. Chung, and I. Yoo, "Performance of threshold switching in chalcogenide glass for 3D stackable selector," in Proc. Symp. VLSI Technol., Jun. 2013, pp. T240-T241.
- <sup>10</sup> W. Kim, H. Lee, B. Kim, K. Jung, T. Seong, S. Kim, H. Jung, H. Kim, J. Yoo, H. Lee, S. Kim, S. Chung, K. Lee, J. Lee, H. Kim, and S. Lee, "NbO<sub>2</sub>-based low power and cost effective 1S1R switching for high density cross point ReRAM application," in Symp. VLSI Technol. Dig. Tech. Papers., Jun. 2014, pp. 1-2.
- <sup>11</sup> S. Jo, T. Kumar, S. Narayanan, W. Lu, and H. Nazarian, "3D-stackable crossbar resistive memory based on field assisted superlinear threshold (FAST) selector," in IEEE Int. Electron Devices Meet. Dig. Tech. papers., 2014, pp. 6.7.1-6.7.4.
- <sup>12</sup> J. van den Hurk, E. Linn, H. Zhang, R. Waser, and I. Valov, "Volatile resistance states in electrochemical metallization cells enabling non-destructive readout of complementary resistive switches," *Nanotechnology* **25**(42), 425202 (2014).

- <sup>13</sup> H. Sun, Q. Liu, C. Li, S. Long, H. Lv, C. Bi, Z. Huo, L. Li, and M. Liu, "Direct observation of conversion between threshold switching and memory switching induced by conductive filament morphology," *Adv. Funct. Mater.* **24**(36), 5679–5686 (2014).
- <sup>14</sup> I. Valov, R. Waser, J. R. Jameson, and M. N. Kozicki, "Electrochemical metallization memories—Fundamentals, applications, prospects," *Nanotechnology* **22**(25), 254003–254024 (2011).
- <sup>15</sup> N. Onofrio, D. Guzman, and A. Strachan, "Atomic origin of ultrafast resistance switching in nanoscale electrometallization cells," *Nat. Mater.* **14**, 440–446 (2015).
- <sup>16</sup> S. Coffa, J. M. Poate, and D. C. Jacobson, "Determination of diffusion mechanisms in amorphous silicon," *Phys. Rev. B* **45**(15), 8355–8358 (1992).
- <sup>17</sup> F. Rollert, N. A. Stolwijk, and H. Mehrer, "Solubility, diffusion and thermodynamic properties of silver in silicon," *J. Phys. D: App. Phys.* **20**, 1148–1155 (1987).
- <sup>18</sup> J. I. Pankove and N. M. Johnson, *Hydrogen in Semiconductors* (Academic press, 1991), Vol. 34.
- <sup>19</sup> M. Hossain, H. H. Abu-Safe, H. Naseem, and W. D. Brown, "Characterization of hydrogenated amorphous silicon thin films prepared by magnetron sputtering," *J. Non-Cryst. Solids* **352**, 18–23 (2006).
- <sup>20</sup> S. Coffa and J. M. Poate, "Hydrogen induced detrapping of transition metals in amorphous silicon," *Appl. Phys. Lett.* **59**(18), 2296–2298 (1991).